Continuous representation of wind stress and wind stress curl over the world ocean

by Alan J. Evenson and George Veronis[1]

ABSTRACT

A continuous wind stress distribution over the world oceans is derived by fitting a spline function representation to the values of the wind stress given by Hellerman (1968) for each season and for the annual mean. The derived wind stress is then used to obtain a representation for the curl of the wind stress over the same region, and steadystate, Sverdrup transport calculations are calculated from the curl for each set of data. The derived transports for the western boundary currents do not agree with observed estimates. They are generally too small in the northern hemisphere and too large in the southern hemisphere. Possible reasons for the discrepancy are discussed.

1. Introduction

When Munk (1950) published his discussion of wind-driven ocean circulation, he pointed out that only a fraction of the observed Gulf Stream and Kuroshio transports could be accounted for by the Sverdrup (1947) transport balance, relating meridional transport in the interior of the ocean to the curl of the wind stress. As possible reasons for the discrepancy, he mentioned: 1) the inadequacy of wind observations; 2) the uncertainty in the drag coefficient for the calculation of wind stress from observed wind data; and 3) contributions due to thermohaline processes.

There are additional possible explanations for the discrepancy. However, before pursuing these possibilities, we decided to try to produce the most representative distribution of the wind stress and the curl of the wind stress over the world's oceans to see how large the discrepancy is between the observed transport and the one calculated from the Sverdrup relation. Hence, starting with the wind stresses obtained by Hellerman[2] (1968) from observed winds and reported at 5° intervals in longitude and latitude, we have used spline functions to obtain a continuous spatial distribution of the stresses for each season and for the annual mean and then we calculated the curl from the continuous distributions for each data set. We then used the steady Sverdrup transport balance

1. Department of Geology and Geophysics Yale University, New Haven, Conn. 06520, U.S.A.

2. Hellerman's 1967 paper lists the same values for each season and for the annual mean. The correct values are given in the 1968 paper.

$$\frac{2\Omega \cos \varphi}{a} V = \frac{1}{\varrho} \boldsymbol{k} \cdot \nabla \times \boldsymbol{\tau} \tag{1}$$

to obtain the meridional transport and finally substituted the transport stream function,

$$\partial \psi / \partial \lambda = aV \cos \varphi \tag{2}$$

in equation (1) and integrated it westward from the appropriate eastern boundary to obtain the transport at each longitude. In the above equations Ω is the angular rotation rate of the earth, λ is longitude, φ is latitude, a is the radius of the earth, $\frac{1}{\varrho} \boldsymbol{k} \cdot \nabla \times \boldsymbol{\tau}$ is the curl of the wind stress per unit mass, V is the meridional volume transport and ψ is the transport stream function.

A spline function representation of the stress field is preferable to more classical representations (least squares polynomials or orthogonal functions) because it provides a very good local fit. With care in choosing the locations of the knots, one can preserve most of the structure (peaks and valleys) so that the smoothing is kept to a minimum. At the same time unusual local features do not affect the behavior at distant points. Once this continuous stress distribution is obtained, one can calculate the curl of the stress and the Sverdrup transport at any point as outlined above. Hence, the maximum structure of the curl of the wind stress and, consequently, of the Sverdrup transport, is preserved.

One useful result of the present calculation is that one can use the continuous spline function representation to calculate any function of the stress at any point. Models of ocean circulation require both the curl of the wind stress and its spatial derivatives. Hellerman's grid is too coarse for this purpose. Our continuous representation for the stress obviously amounts to an interpolation between the grid points of the observed network but that is what one must do if a denser network of values is required. Our feeling is that we have made use of the spline function method to obtain a continuous distribution that yields maximum agreement with Hellerman's values and that the continuous distribution is the most reasonable interpolation that one can make. We can thus determine whether the western boundary transports deduced from the Sverdrup relation agree with the observed values.

Our procedure provides no test of Hellerman's data *per se*. It is possible that a denser array of observed values or a better determination of the stress from the observed winds would lead to a more rigorous test of the transport question but we have not probed into that part of the problem.

The conclusions that emerge from the calculated wind stress and the resulting curl fall into two categories, one having to do with comparison with earlier calculations and the other with the implications of the results themselves.

First, at the outset of our investigation we were concerned primarily with the task of obtaining a reasonable estimate of the wind stress and its spatial derivatives

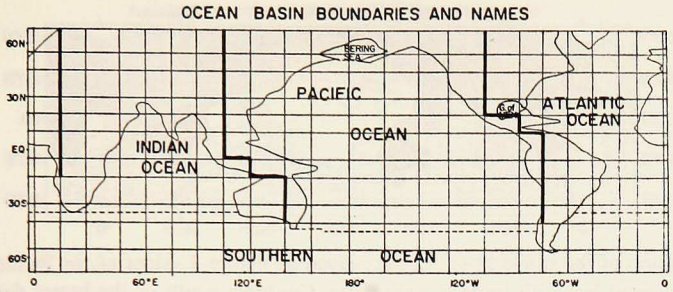

Figure 1. Continental boundaries for the world as used for the computations on a mapping using equally spaced for longitude and latitude. Shallow water areas (north of Australia and the Caribean) appear as land. The dashed lines in the southern hemisphere form the northern boundary of the Southern Ocean. The heavy black lines are the fences referred to in the text.

in any region and at any time for which observed data seemed adequate. Hellerman's data is reported at five-degree intervals in longitude and latitude over almost the entire ocean surface south to 50°S. Poleward of this latitude the data is sometimes too sparse for the purposes at hand, particularly for the winter season in the southern ocean. The northern boundary of the region for which the calculated values are unreliable is marked with a dashed curve in each data set.

In the remaining regions the reliability of the calculated values is limited mainly by the density of Hellerman's grid. Obviously, no calculation can yield meaningful structure with a scale smaller than that of the observed values. However, a good interpolation scheme *can* provide more detail for the derivatives than can be obtained by taking finite differences of the observed values.

To shed light on this point we have compared our results for the annual mean of the curl with those obtained by Stommel (1964) and by Hantel (1971). Stommel's calculation is based on Hidaka's (1958) wind stress data and is confined to a smaller band of latitudes but much of that data was also used by Hellerman so that the derived distributions of the curl should agree at least qualitatively in the regions

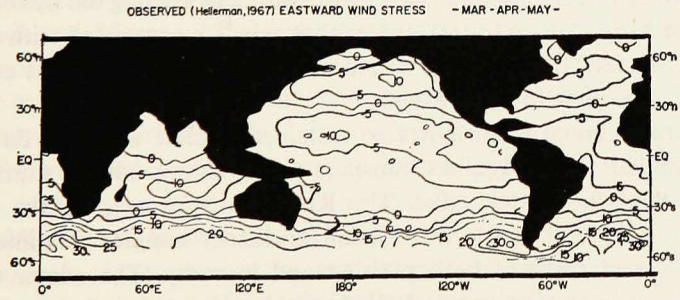

Figure 2. Hand-drawn contours of the eastward wind stress over the world oceans during the spring season from data by Hellerman (1968). There is no data over most of the oceans south of 50°S. Units are 10^{-1} dynes/cm^2.

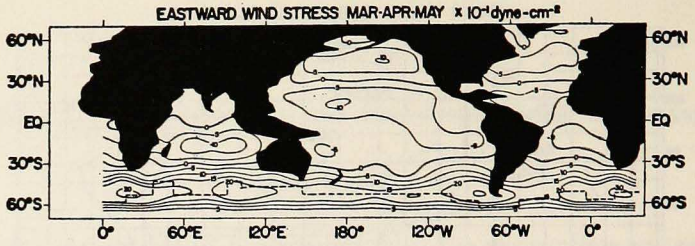

Figure 3. Contours of the spline fit to the data given in Figure 2. Most of the features of Figure 2 appear here as well but with smoother structure. Contours south of the heavy dashed curve are extrapolations and are not quantitatively significant. Units are 10^{-1} dynes/cm^2.

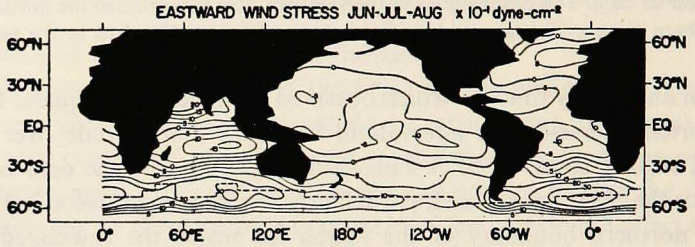

Figure 4. Contours of the spline fit to Hellerman's (1968) wind-stress data for the summer season. Units are 10^{-1} dynes/cm^2.

of overlap. Our calculations agree reasonably well with both Hantel's and Stommel's although, as we expected, the curl in the present calculations shows more structure. In places our maximum magnitudes are greater than theirs (by as much as a factor of two in some areas) and we obtain larger differences in both longitude and latitude within each ocean basin. The same statements apply when we compare our calculations for the seasonal curl with those reported by Hantel (1971).

Using the curl distributions obtained in this manner, we then calculated the Sverdrup transport and the associated transport stream function ψ, for each data set. Distributions of ψ are shown in Figs. 14 to 18. The western boundary transports obtained by these calculations are given by the values of ψ along the western boundary of each ocean basin. The only ambiguities that arise are associated with the question of whether a surface feature, such as New Zealand, is to be treated as an eastern boundary of limited latitudinal extent.

The western boundary transports so obtained exhibit seasonal fluctuations of different magnitudes. The Agulhas transport during the (southern) summer is about 30% larger than the winter value. The Kuroshio transport, on the other hand, increases by a factor of nearly three from (northern) summer to winter. The East Australian Current shifts in both position and intensity. The winter transport of the Gulf Stream is approximately 50% larger in winter than in summer and fall.

Given such results how are we to interpret steady-state calculations of ocean circulation based on time-averaged stresses and curls? And with what are the results

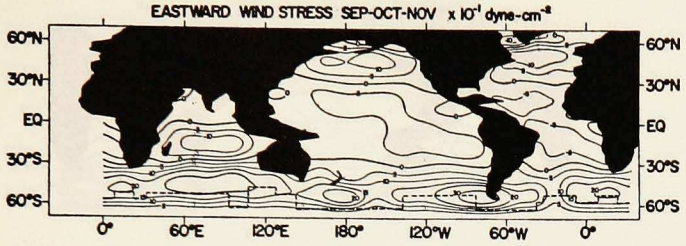

Figure 5. Contours of the spline fit to Hellerman's (1968) wind-stress data for the autumn season. Units are 10^{-1} dynes/cm^2.

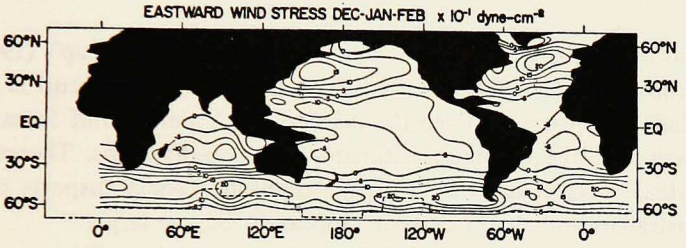

Figure 6. Contours of the spline fit to Hellerman's (1968) wind-stress data for the winter season. Units are 10^{-1} dynes/cm^2.

of these calculations to be compared? Estimates of transports of western boundary currents are based on observations taken at specific times and are representative of transports during more pleasant local observational conditions. Do these transport values reflect oceanic response to intense forcing during winter or to weaker summer winds?

We have some theoretical basis (Veronis and Stommel, 1956) for expecting only mild baroclinic response of the ocean to winds that vary on a seasonal time scale. Even though bottom topography can generate a baroclinic response from barotropic modes, we do not know enough of this mixing of modes for realistic time and space scales associated with wind forcing and bottom topography to be able to predict the detailed response for the general circulation. However, since calculations (Ichiye, 1950; Veronis and Morgan 1955) indicate that the western boundary current in a barotropic ocean of uniform depth responds very quickly to transient winds in the interior, we can expect the effects of the fluctuations to be reflected in the western boundary transports. Whether the major response is barotropic or baroclinic is important for transport estimates based on observations because the latter rely on geostrophic calculations, often with no fixed reference point that would make it possible to identify the barotropic transport.

Even if we were able to resolve the issues mentioned above, the fact remains that our transport calculations produce values that are generally not in good agreement with observed estimates. The maximum calculated transport of 58 sverdrups[3] for

3. 1 sverdrup = 10^6 m^3/sec.

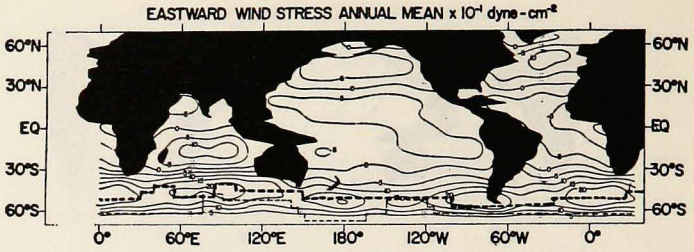

Figure 7. Contours of the spline fit to Hellerman.s annual mean wind stress data. Units are 10^{-1} dynes/cm^2. The heavy dashed line marks the limit south of which data is missing for at least one season. South of the light dashed line there is no data.

the Kuroshio occurs in winter and is nearly as large as Sverdrup's (1942) estimate of 65 sverdrups. The transport deduced from the annual mean curl is just slightly more than half the observed. Even the *maximum* calculated Gulf Stream transport is much lower than the minimum estimates from observations. Theoretical values for the Agulhas Current are of the right magnitude. The transports obtained for the East Australian and Brazil currents appear to be too large.

Since the oceans are driven by differential heating and cooling as well, we may expect quantitative modifications to the calculations made above. Stommel's (1965) estimate of the thermohaline circulation for the Atlantic showed how the upper layer transport of the Gulf Stream can be enhanced and that of the Brazil Current reduced by a thermohaline circulation superimposed on the wind-driven one. A similar calculation can be made for the Pacific, although the intensity of cooling in the North Pacific is much reduced so that the correction would presumably be smaller[4].

In addition to the above, we know from both observations and theoretical calculations that there can be a substantial (inertial) recirculation in the form of a closed anti-cyclonic circulation just offshore of the western boundary currents near the latitude of maximum transport. This recirculation would not show up in a simple calculation based on the Sverdrup transport, i.e., it would not appear in the determination of the *net* transport. However, it may affect the estimates made from observed data since the measurements themselves are often terminated at the offshore point where the observer feels that the transport has leveled off. Hence, the observed estimates may include the downstream part of a very intense recirculation and the *net* transport could then be seriously overestimated. The question that arises in this connection is: are observers and theoreticians talking about the same quantity when they attempt to compare theoretical and observed values of the transport of a western boundary current?

The issues that we have raised in the foregoing remarks are ones that must be faced eventually for models of large scale ocean circulation but they do not affect the specific purpose of the present calculations. Our aim has been to develop the

4. Either that or the return of denser water may take place at an intermediate level, i.e., not as abyssal water, and exactly how that would affect "upper" layer transport is not clear.

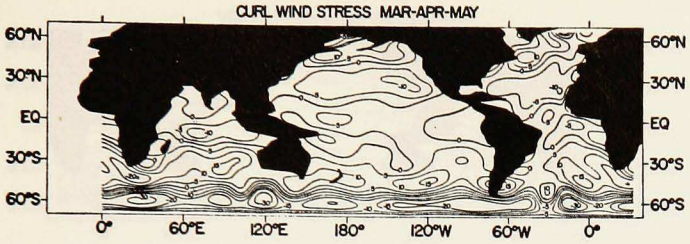

Figure 8. Wind stress curl over the world ocean for the spring season as calculated by the spline function method. Units are 10^{-9} dynes/cm^3.

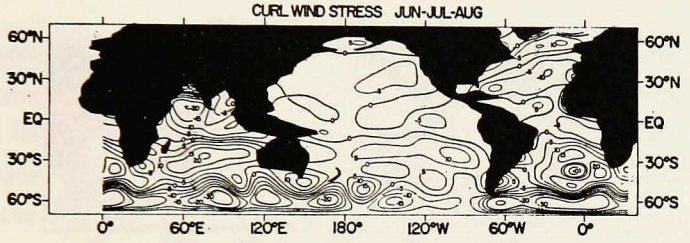

Figure 9. Wind stress curl over the world ocean for the summer by the spline function method. Units are 10^{-9}/cm^3.

best continuous representation of the wind stress that we can from a world-wide network of values based on observed winds and to present a scheme for obtaining first and second derivatives of these stresses at any desired point. The specific results of these calculations are presented and discussed below along with the calculations of the stream function based on Sverdrup transports.

Because of the rather substantial effort required to generate the continuous distributions from the observed values, we have produced a magnetic tape containing the program so that it is available to anyone who wishes to make use of it. The Director, National Climatic Center, Federal Building, Ashville, North Carolina 28801 has generously agreed to handle requests for the tape and anyone wishing to obtain the tape can write to that address for a copy.

2. The spline function representation

In principle, obtaining a spline function representation for a given set of data points is equivalent to a least squares fit. The difference in practise is that the spline functions are locally low-order polynomials that are non-zero only within an interval whose size is determined by the order of the polynomial. Thus, a linear spline function between the points x_{i-1}, x_i and x_{i+1} is zero for $x \leq x_{i-1}$, increases linearly to a peak at x_i, decreases linearly from x_i to x_{i+1} and vanishes for $x \geq x_{i+1}$. A cubic spline associated with point x_i is non-zero only over the interval x_{i-2} to x_{i+2}. The basic spline functions are normalized over the range of definition.

To obtain a spline fit for a one-dimensional system, it is advisable first to plot

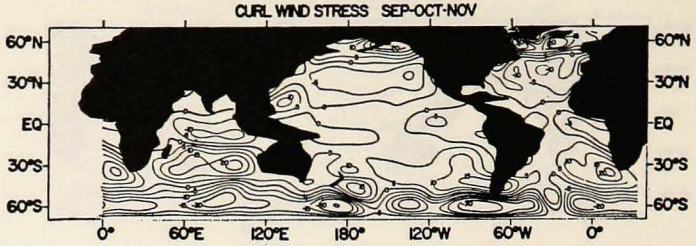

Figure 10. Wind stress curl over the world ocean for the autumn season as calculated by the spline function method. Units are 10^{-9} dynes/cm^3.

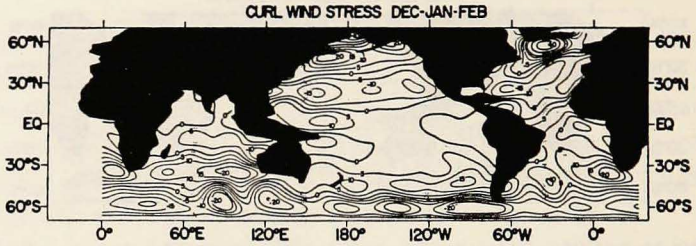

Figure 11. Wind stress curl over the world ocean for the winter season as calculated by the spline function method. Units are 10^{-9} dynes/cm^3.

the data in order to determine the amount of structure present. Then points, called knots, are marked off at, or near, apparent extrema so that the data set is divided into (generally) unequal segments each of which represents a local "half wavelength" of the data set. The knots are identified with the x_i mentioned above, so that a single spline function (also called a basis function) will normally span a number of points at which data is given. The functional representation of the data is thus given by $\hat{S}(x) = \sum a_i B_i(x)$ where the $B_i(x)$ are the normalized basis functions, the a_i are their coefficients and the summation is taken over the non-zero basis functions at the point x. As in a least squares fit, the a_i are determined from

$$\sum_{n=1}^{N} a_i B_i(x_n) B_j(x_n) = \sum_{n=1}^{N} S(x_n) B_j(x_n) \tag{3}$$

where $S(x_n)$ is the actual data value at the point x_n and N is the total number of data points.

The larger the degree of the spline polynomial, the smoother the final representation. Thus, linear splines approximate the data by straight line segments between knots but cubic splines lead to continuous second derivatives everywhere. The computational effort increases with the degree of the polynomial and with the number of knots used. As with all such approximations a balance must be struck between the amount of detailed behavior sought and the ease and reasonableness of the computation. Also, for a given number of data points, if the degree of the polynomials

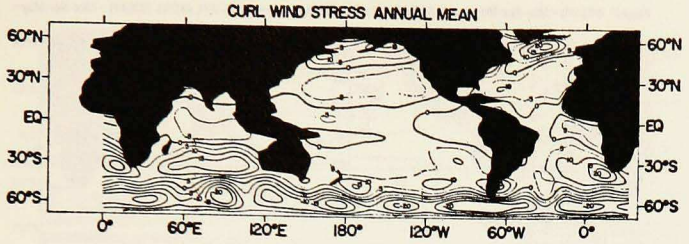

Figure 12. Annual mean wind stress curl over the world ocean as calculated by the spline function method. Units are 10^{-9} dynes/cm^3.

is too high or if the number of knots is too large, the system may become ill-conditioned and lead to unreliable results.

For two dimensions the normal procedure for a convex region is to solve the two-dimensional form of equation (3) for the coefficients a_i. Then the calculated function is given by

$$\hat{S}(x,y) = \sum a_i B_i(x,y) \tag{4}$$

where the summation is taken over all basis function which are non zero at (x,y). In the present calculations x and y are replaced by longitude, λ, and latitude, φ.

To approximate the distribution of wind stress given by Hellerman (1968) we used products of cubic B-splines[5] in latitude and longitude.

The latitude band $-68° \leq \varphi \leq 68°$ included 12 knots located at $-68°$, $-55°$, $-40°$, $-30°$, $-15°$, $-5°$, $10°$, $20°$, $30°$, $45°$, $55°$, $68°$. The same latitude locations could be used for the knots in all of the ocean basins. In longitude 22 knots were used, the locations of which are measured in degrees eastward of the Greenwich meridian: 0°, 15°, 30°, 50°, 65°, 80°, 95°, 110°, 125°, 145°, 160°, 180°, 200°, 220°, 235°, 255°, 275°, 290°, 305°, 320°, 335°, 345°. The smallest scale of resolution is a half wavelength of 10° in both latitude and longitude.

The basis functions in each direction are cubic polynomials between knots and are identically zero at and beyond $\pm$ 2 knots from the "central" knot with which the function is identified. Each function is normalized over all space, and the representation is continuous and has continuous first and second derivatives. The two-dimensional basis function associated with the intersection of the knots in longitude and latitude is the product of the one-dimensional functions associated with the intersecting knots.

Since the world ocean is not bounded by a convex region, the procedure was modified by the introduction of additional lines, which we call fences and across which the stress may be discontinuous. These fences, shown in Fig. 1, serve to "disconnect" the stresses in one basin from those on the other side of the fence. Thus, if a basis function in the Atlantic near the South American fence is defined

5. In spline theory the term B-spline refers to a polynomial that vanishes outside a certain interval and is positive definite within that interval.

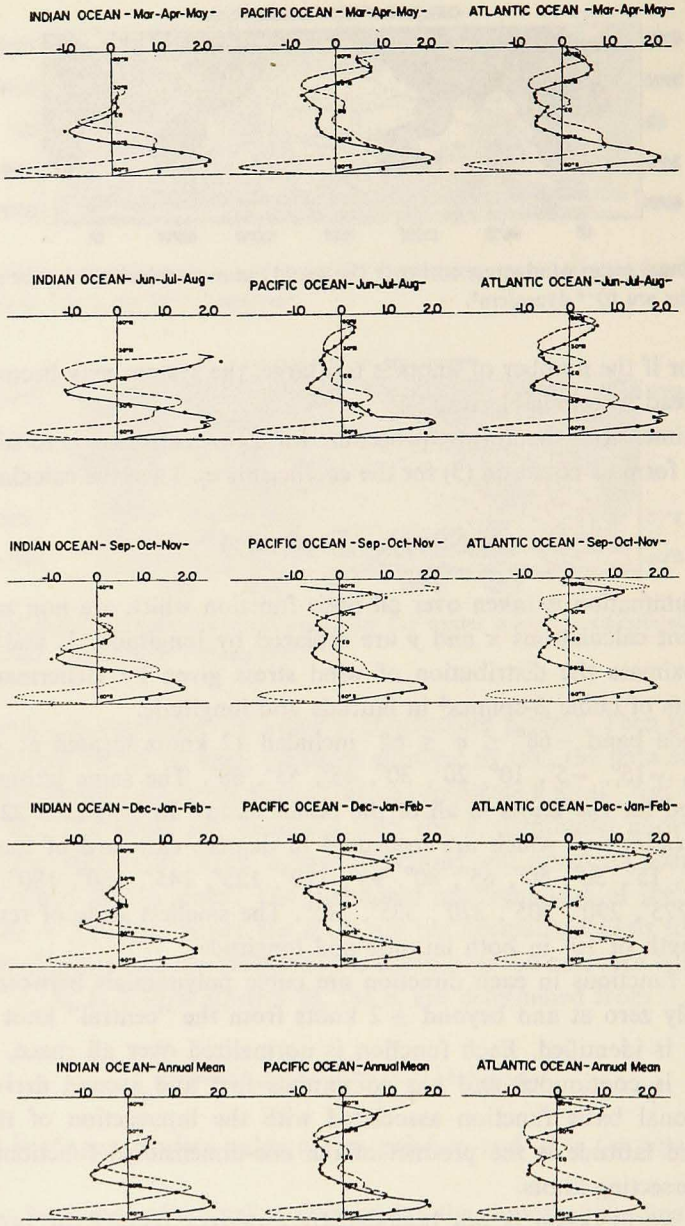

Figure 13. Seasonal averages and mean values of eastward wind stress averaged zonally for each ocean are shown by black dots (black squares for the Southern Ocean) for observed values and by the solid curves for the spline representation. The zonally averaged calculated wind stress curls are shown by the dashed curves. The stress is in units of dynes/cm^2 and the curl is in units of 10^{-8} dynes/cm^3. The apparent breaks in the wind stress values and in the curves occur at the latitude where the Southern Ocean begins (the longitudinal extent of the Southern Ocean being larger than that of the oceans north of it).

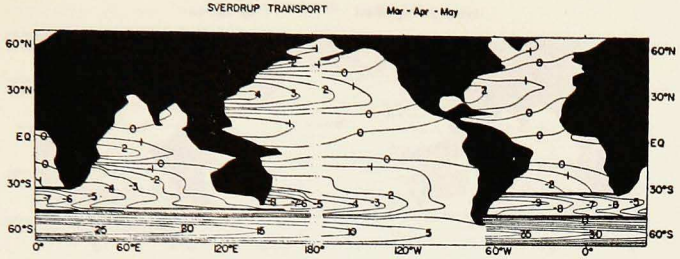

Figure 14. Contours of the transport stream function, ψ, for the spring season obtained by integrating equation (2) westward from the eastern boundary of each ocean basin. The maximum values at the western sides of the basins are the calculated transports for the western boundary currents. Units of ψ are 10^7 m^3/sec.

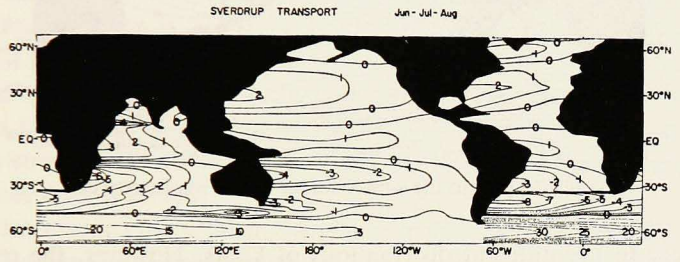

Figure 15. ψ from the summer values of the wind stress curl.

over a north-south interval that does not project south of 45°S its values on the Pacific side of the fence are set equal to zero. Hence, the calculated value at a point in the Atlantic depends only on values in the Atlantic. If a basis function is defined in an interval extending poleward of the end of the fence, e.g., near the southern tips of Africa, South America and Tasmania, the stress values on one side of the fence influence the calculated values on the other side.

We thus obtained a spline fit for the eastward and northward components of wind stress, τ^λ and τ^φ. The curl of the wind stress, $\boldsymbol{k} \cdot \nabla \times \boldsymbol{\tau}$, is given by

$$\boldsymbol{k} \cdot \nabla \times \boldsymbol{\tau} = \frac{1}{a \cos \varphi} \frac{\partial \tau^\varphi}{\partial \lambda} - \frac{1}{a} \frac{\partial \tau^\lambda}{\partial \varphi} + \frac{\tau^\lambda}{a} \tan \varphi. \tag{5}$$

Hence, spline fits were obtained for $S_1 = \tau^\lambda$, $S_2 = \tan \varphi \, \tau^\lambda$, $S_3 = \tau^\varphi / \cos \varphi$ and the coefficients of these fits were then used in (5) to obtain the curl of the wind stress. The curl so obtained is continuous and has continuous first partial derivatives everywhere.

The different sets of data that were to be approximated had structure that could be described with the number and placement of knots listed above. Had the structure differed drastically, particularly in scale, from one set to the other, it might have

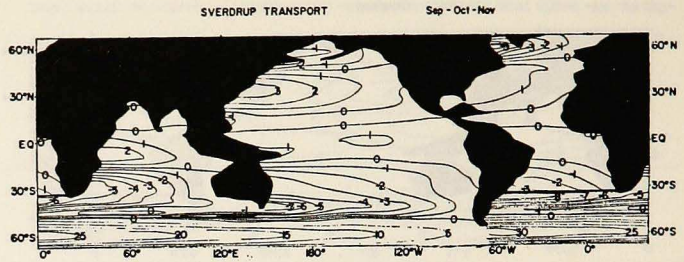

Figure 16. ψ from the autumn values of the wind stress curl.

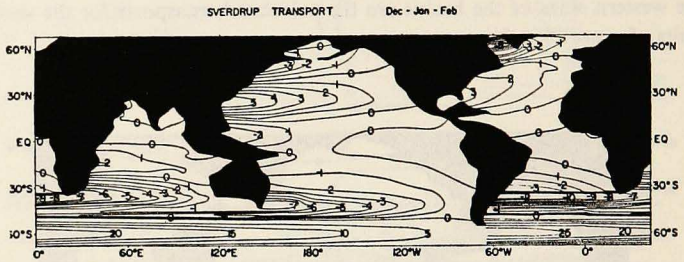

Figure 17. ψ from the winter values of the wind stress curl.

been necessary to use different distributions of knots. However, the reliable detail in the observed network is of sufficiently large scale that such a refinement is not necessary.

3. The calculated representations

Fig. 1 shows the basic map on which the results are displayed. The land-water boundaries are smoothed and certain features such as the various Indonesian seas and the Caribbean are imbedded in fictitious land masses. The projection is not conformal but consists of equally spaced units for longitude and latitude. The Atlantic, Pacific, Indian and Southern oceans are delimited by the bordering land masses and by the dashed line the location of which is determined by the southern projection of a land mass that serves as a boundary for that ocean. Thus, the southern boundary for the Atlantic and Indian oceans is the southern tip of Africa (36°S) and the corresponding boundary for the Pacific.is the south tip of New Zealand (48°S). Also the locations of the fences are shown as heavy lines mostly running north south.

To indicate how well the observed and calculated distributions agree we show in Fig. 2 the distribution of eastward stress as it appears when contoured by hand, using Hellerman's values at 5° intervals, and in Fig. 3 the calculated distribution according to the spline fit. The two are very similar, as they should be, but the spline representation is smoother with somewhat smaller extreme values and a less wiggly structure. As is normal with hand contouring, details of the distribution reflect the

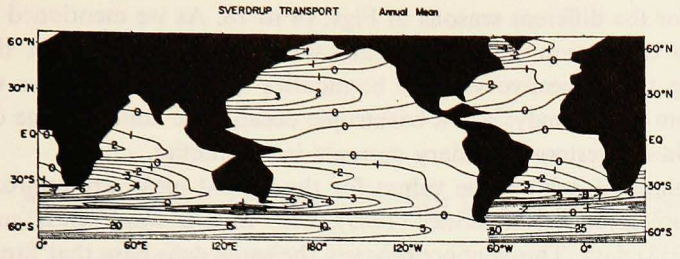

Figure 18. ψ from the annual mean winter stress curl.

judgement of the draftsman. The minor differences in detail should not lead to significant differences in calculated derivatives etc.

The eastward stresses for the remaining seasons are shown in Figs. 4 to 6 and that for the annual mean is in Fig. 7. In all of the distributions the paucity of data south of 50°S or so makes the results unreliable. In order to arrive at reasonable values for the wind stress and curl south of 50°S it was necessary to impose a boundary condition on the spline fit that the wind stress and first partial derivatives vanish at 68°S. The stress condition can be partially justified since that appears to be the trend whenever data is present.

The main features to emerge from the graphs include the relatively rich structure in the North Atlantic and Pacific during the winter season and the weaker stresses in those basins during spring and summer. The Indian Ocean, on the other hand, has greater stresses during northern summer (the monsoon season). The map for the annual mean stresses exhibits greater uniformity zonally than does the winter map but comparable to that for the spring.

The calculated distributions of the curl of the wind stress for the four seasons and the annual mean are shown in Figs. 8 to 12. On the whole, there is more zonal variability in the curl than in the eastward stress. The most significant result, however, is the substantial variation in the amplitude of the curl from winter to summer in the North Pacific. A comparison with Hantel's charts reveals the larger peak values obtained for the curl from the spline function fit. These larger values lead to larger transports.

Fig. 13 contains the zonally averaged eastward wind stress for observed values (black dots) and from calculation (solid curves) as well as the zonally averaged curl (dashed curves) for each ocean basin for each season and for the annual mean. The Southern Ocean curves join those of the respective basins across the breaks. The indicated discontinuities occur because of the different longitudinal ranges for the zonal averages. Generally, the Southern Ocean values are averaged over a larger longitude range than those of the individual ocean basins as can be seen from Fig. 1. These zonal averages exhibit the seasonal variability at a glance. The close fit of observed and calculated data is also evident in this figure.

Finally, we show the distributions of the transport stream functions for the world

ocean and for the different seasons in Figs. 14 to 18. As we mentioned in the introduction, the calculation was made from steadystate dynamics but the transport values along the respective western boundaries is indicative of the values to be expected from linear analysis of a barotropic ocean. The annual range of transports in the individual western boundary currents is substantial.

In the regions of overlap the values for the annual mean are approximately the same as those given by Welander (1959), who used a wind stress curl based on Hidaka's (1958) data. This is approximately the same data base that Stommel (1965) used to obtain the curl distribution.

The significant increase of transport in the anti-cyclonic gyres of the North Atlantic and Pacific during winter are evident. Whether these transports are more representative of the circulation is a question which remains unanswered and which we have discussed in the introduction.

Acknowledgement. Support by the National Science Foundation under grants GA40705-X and DES 73-00424 A01 is gratefully acknowledged.

REFERENCES

Hantel, M. 1972. Wind stress curl – the forcing function for oceanic motions. *Studies in Physical Oceanography*. Ed. Arnold Gordon. Gordon and Greach. New York. 194 pp.

Hellerman, S. 1968. An updated estimate of the wind stress on the world ocean. *Monthly Weather Review*, 96, 67–74.

Hidaka, K. 1958. Computation of the wind-stress over the oceans. *Geophysical Notes* 11, 77–123.

Ichiye, T. 1951. On the variation of ocean circulation. The Oceanographic Magazine, 3, No. 2.

Munk, W. H. 1950. On the wind-driven ocean circulation. *J. Meteor.*, 7, 79–93.

Stommel, H. 1964. Summary charts of the mean dynamic topography and current field at the surface of the ocean, and related functions of the mean windstress. Studies in Oceanography, Ed. K. Yoshida. University of Washington Press. Seattle. 568 pp.

Stommel, H. M. 1965. The Gulf Stream. Univ. of California Press. Berkeley. 248 pp.

Sverdrup, H. V. 1947. Wind-driven currents in a baroclinic ocean; with application to the equatorial currents of the eastern Pacific. Proc. Nat. Acad. Sci. Wash., 33, 318–326.

Veronis, G. and H. M. Stommel. 1956. The action of variable wind stresses on a stratified ocean. J. Mar. Res., 15, 43–75.

Veronis, G. and G. W. Morgan. 1955. A study of the time-dependent winddriven circulation in a homogeneous, rectangular ocean. Tellus, 7, 232–242.

Welander, P. 1959. On the vertically integrated mass transport in the oceans. The Atmosphere and the Sea in Motion. Ed. Bert Bolin. The Rockefeller Institute Press. New York. 509 pp.

Received: *15 January 1975.*